hydrides, Si_2H_n, where n = 0-6 and $Si_2H_n^+$, where n = 0-7. The calculated thermodynamic properties of the neutral species were in agreement with experimental data reporting the existence of stable silicon hydrides having n values of 2-5.

An interesting study was made in collaboration with the Central Institute of Inorganic Chemistry, Berlin, Germany, on $MAlF_4$ complexes where M = H, Li, or Na. These complexes are involved in high-temperature industrial processes, catalysis, chemical synthesis, and metal halide lamps. Investigations were conducted on the three structures shown in Fig. 6-36, in which the Al-M atoms are bridged at the corners, edges, or faces of the structure. Edge and corner bridging in $HAlF_4$ are of about equal energy (0.4 kJ/mol); $LiAlF_4$ has an edge-bridged structure; and the edge- and face-bridged structures of $NaAlF_4$ are of nearly equal stability. The $HAlF_4$ complex is much less stable than the alkali complexes, which may be a reason why difficulties have been encountered in observing this molecule.

In 1992, the CMT Annual Report stated that "The Gaussian-2 (G2) theoretical procedure, developed in a collaborative effort with AT&T Bell Laboratories and Carnegie Mellon University, is beginning to receive (1) wide acclaim for its accuracy in calculating molecular energies, and (2) extensive use in the field of computational chemistry." The G2 theory was being used widely by universities and industry for calculations of thermochemical data. The method is accurate to ±2 kcal/mol for calculating reaction energies. In 1992, the procedure was used in the modeling of thin-film diamond growth mechanisms, based on carbon dimer as the growth species. The model involved the formation of diamond-like carbon clusters by reactions of carbon with hydrocarbons.

By 1995, the G2 procedure had been extended to the elements Ga→Kr of the third row of the periodic table. Spin-orbit corrections for atoms and molecules having partially degenerate states were included explicitly in the G2-calculated energies. The average absolute deviation from experimental values for 40 test reactions was 1.37 kcal/mol.

An enlarged G2 neutral test set of 148 molecules was used to assess the performance of the G2 theory and two modified versions of it, G2(MP2) and G2(MP2,SVP). The mean absolute deviations for the three theories were 1.58, 2.04, and 1.93 kcal/mol, respectively. All three theories achieve the desired chemical accuracy of 2.0 kcal/mol. The modified versions, G2(MP2) and G2(MP2,SVP), are slightly less accurate than the original G2 theory, but they require significantly less computer time and disk space.

Personnel. Larry Curtiss was the Division's leader in this area. Some of the others who had a particular interest in this work were Milt Blander, Vic Maroni, Chris Marshall, Zoltan Nagy, Jerry Rathke, Marie-Louise Saboungi, and Shiu-Wing Tam.

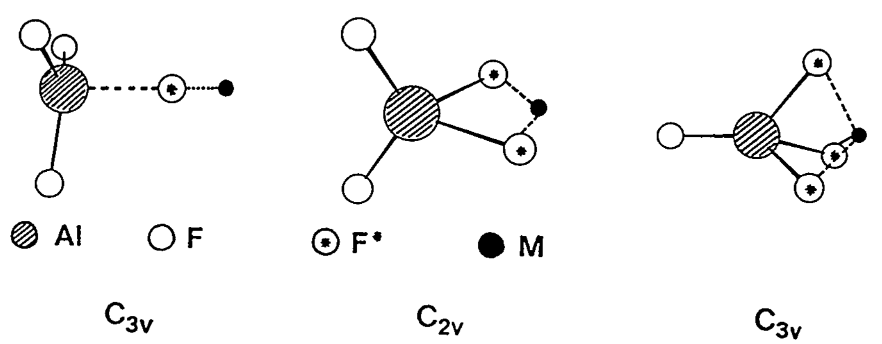

Fig. 6-36. Illustration of $MA1F_4$ Structures

MOLECULAR SIEVE RESEARCH

Advances in the synthesis of novel molecular sieve materials had paved the way for product-selective catalysis in the processing of fuels and chemical feedstocks. The CMT work in this area consisted mainly of theoretical studies of molecular sieve synthesis. Much of this work was based on the type of molecular orbital calculations discussed in the preceding section.

Ab initio molecular orbital calculations and inelastic neutron scattering techniques were used to determine the effects of the molecular sieve framework on the vibrational frequencies and rotational diffusion of occluded template molecules. The potential energy surface of tetraethyl-ammonium cation for rotation about the C-C and C-N bonds showed no distinct configurations that corresponded to local minima of approximately equal energy. Another study was made to investigate the Brønsted acidity of $Si_n(OH)_m$ clusters similar to those in molecular sieves. Proton affinities, which are an important factor in defining Brønsted acidity, were calculated with accuracies of 5-10%. This made possible a direct correlation of calculated O-H bond strength with observed catalytic activity.

The characteristics of clusters containing up to 160 atoms were calculated by the G2 theoretical procedure—some of the largest clusters ever used in electronic structure calculations on zeolites. Proton affinities, ammonium-ion affinities, and ammonia desorption energies were determined for these clusters. The calculated values for the properties of zeolites and molecular sieve materials were in good agreement with experimentally determined values that were available.

Continuing studies produced two significant findings. First, the energetics of the Brønsted acid site in TSi_nO_m clusters, where T = Si or Al, that have zeolite-type structures were calculated, and key properties of structures that are strongly correlated with the acid catalyst performance of zeolite materials were determined with unprecedented accuracy. Second, zeolite frameworks having sulfided metal clusters in void regions of the crystal structure were found to catalyze the conversion of methane to higher hydrocarbons. The reaction rates were low, but the selectivity to produce C_{2+} hydrocarbons was close to 100%.

In the hydrocarbon cracking process used by the petroleum industry, proton transfer between the adsorbed molecule and the zeolite catalyst was known to be a key mechanism. To understand the energetics of proton transfer and acid catalysis in zeolites, the equilibrium geometries of protonated alkanes (carbonium ions) were investigated, and their proton affinities were calculated using the G2 theory. For protonated ethane, the calculated proton affinity of the lowest energy structure was 141.0 kcal/mol, which agreed well with the experimental value of 139.6 kcal/mol. Proton transfer from the Brønsted acid site to an adsorbed molecule was believed to be a key mechanism not only for hydrocarbons, but also for other molecules such as water, ammonia, and methanol. In the case of water, the structure resulting from proton transfer to an adsorbed water molecule was found to exist only as a transition state, but the adsorption of a second water molecule stabilized the proton transfer structure, creating a local minimum in the potential energy surface (a more stable arrangement). The study was then extended to the interaction of the water dimer with the acid site in the zeolite ZSM-5 to a five-metal atom cluster ($AlSi_4O_4H_{12}$) model. Equilibrium geometries of the neutral $[ZH...(OH_2)_2]$ and ion-pair $[Z^-...H(OH_2)_2^+]$ adsorption complexes were calculated, as well as the transition geometries between these two species. Density function theory was used for these calculations. While not quite as accurate as G2 theory, it is more cost-effective. The relative energies of the two species and the transition state were small, indicating free movement of the proton.

Recent work in this area had shown some particularly noteworthy results on interactions of ethane with zeolite clusters. The $H_3SiO(H)Al(OSiH_3)_4$ cluster model, which includes five tetrahedral atoms, allows an adsorbed molecule to interact with three oxygen atoms adjacent to the substituted aluminum site. Calculations have identified several stationary points on the potential energy surface for the interaction of methane with the zeolite acid site (ZH). The calculations provide evidence for the existence of a stable ion-pair structure ($Z^-...C_2H_7^+$), whose existence had been contested. In addition, a new calculated value for the proton transfer barrier from the zeolite to the adsorbed hydrocarbon is in much closer agreement with typical experimental values than had been obtained previously.

Personnel. This work was done by Vic Maroni, Larry Curtiss, L. Hon, and Stan Zygmunt (an STA).

ELECTROCHEMICAL AND CORROSION STUDIES

Spectroelectrochemical and Synchrotron Studies. As mentioned earlier, a combination of spectroscopic and electrochemical techniques can be highly synergistic in understanding the detailed mechanisms of corrosion reactions and other chemical processes. The spectroelectrochemical investigations described in this section used a battery of such techniques: (1) laser Raman and UV-visible spectroscopy to determine *in situ* the structures and compositions of anodically formed corrosion films on metals, (2) photoelectrochemical and ac impedance measurements to characterize the electronic band structures of the films and to study their transport properties and conduction mechanisms, and (3) ac and dc polarization, cyclic potentiodynamic sweeps, and other transient techniques to examine the interfacial processes involved in metal corrosion. The synchrotron studies in this program were collaborative efforts with outside organizations, including Exxon Research and Engineering Co., the Naval Surface Warfare Center, the University of Poitiers in France, the University of Auckland in New Zealand, and members of the ANL Materials Science Division. Some of the research in this area was oriented toward possible future use of the Advanced Photon Source, which was under construction at ANL.

Surface enhancement of Raman scattering (SERS) by electrodeposition of silver showed that the passive films on iron consist of an inner layer of Fe_3O_4 and $Fe(OH)_2$ and outer layers of α-Fe_2O_3 and FeOOH, depending on the potential. Small amounts of thiocyanate (SCN^-) were found to break down the passivating oxidic layers on iron by complexing Fe^{2+} and Fe^{3+} ions, with subsequent precipitation of iron thiocyanate phases. At thiocyanate concentrations below about 0.001 *M*, however, the iron oxide films were self-healing, thereby preventing catastrophic breakdown. A similar study of the passive film formed on nickel showed that the film was composed of both $Ni(OH)_2$ and NiO, probably as a bilayer structure with the NiO closer to the metal. In subsequent studies at temperatures from ambient to 95°C, $Fe(OH)_2$ and Fe_3O_4 formed in the prepassive region, while Fe_3O_4 and FeOOH predominated at passive potentials.

In the case of chromium, a near-monolayer oxide film of Cr_2O_3 was formed. At more positive potentials (>0 V *vs.* the saturated calomel electrode), there was evidence of Cr(VI) in the form of a soluble chromate. A copper electrode in NaOH solution at -0.05 V *vs.* the standard calomel electrode formed a surface film of Cu_2O. Other work on copper involved studies of electrochemically induced pitting and morphological studies of its electrodeposition, and the behavior of copper in dilute solutions of cyanate (OCN^-) and thiocyanate (SCN^-) in perchlorate supporting electrolyte.

X-ray near-edge spectroscopy (XANES) and extended X-ray absorption fine structure (EXAFS) studies were made on the higher oxide forms of nickel (β-NiOOH, γ-NiOOH, and NiO_2). These materials were of interest both for corrosion protection and as battery electrode materials, and there was confusion in the literature as to the structure and valency of the nickel in these compounds. X-ray absorption measurements showed that all three of the higher oxide forms of nickel had the same disordered, layered structure, which can be represented as NiO_2H_x ($0 < x < 2.0$). Spectroscopic results indicated that the β and γ forms of NiOOH should be regarded as Ni^{3+} compounds. In subsequent studies, synchrotron X-ray absorption was used to characterize further the various phases that could be formed during corrosion of the metal or during the cyclic charging and discharging of nickel electrodes in batteries. The compounds that were characterized included NiO, α- and β-$Ni(OH)_2$, β- and γ-NiOOH, $Ni_3O_2(OH)_4$, NiO_2, Ni_3O_4, Ni_2O_3, and $KNiO_6$. Three distinct Ni-O bond distances were characteristic of Ni^{2+}, Ni^{3+}, and Ni^{4+}. In other work on nickel, an electrochemically deposited nickel oxide film on graphite was discovered to increase the capacitance of the graphite fourfold.

In situ laser Raman spectroscopy was used to investigate the compositions and structures of anodic corrosion films on titanium in various aqueous environments (H_2SO_4, Na_2SO_4, H_3BO_3-$Na_2B_4O_7$, and NaCl solutions). Bands characteristic of the anatase form of TiO_2 were observed at highly anodic potentials, while a disordered amorphous film was formed under cathodic conditions.

Synchrotron-generated far infrared radiation studies of water adsorbed on gold or platinum crystals permitted detection for the first time of the hindered translational mode of water and suggested the formation of water clusters at low coverage and an ice-like layer at higher coverages. Continuing studies showed that water adsorbed molecularly and non-dissociatively on the single-crystal platinum (111) under ultra-high vacuum and low temperatures (< -73°C). The far infrared spectrum of water on Pt (111) was very similar to that of gold.

Electrode Structure and Kinetics Studies. This research was concentrated on the electrode kinetics and atomistic mechanisms involved in metallic corrosion in aqueous solutions over a wide range of temperatures and pressures. This was a new area of investigation, since very little electrode kinetics research had been performed at temperatures over 60°C and practically none above 100°C in aqueous solutions. Much of the interest in aqueous corrosion at higher temperatures and pressures stemmed from corrosion effects in light water reactors (LWRs). The corrosion processes are electrochemical in nature and involve anodic dissolution of the metal together with the reduction of some component of the aqueous solution, such as dissolved oxygen. In reactions of this type, the essential elementary step is the charge transfer between the solid surface and the solution species at the interfacial solution layer (the "interphase"). The kinetics of the charge-transfer step are influenced by the molecular structure of the interphase and potential gradients within it. The electrode kinetics measurements were made by a combination of techniques, including galvanostatic, coulostatic, or potentiostatic pulse transients; ac capacitance methods; and rotating disk-electrode techniques.

Earlier work had shown that a simple charge-transfer reaction does not behave anomalously at high temperatures, so discrepancies reported in the literature must have been caused by something else. The ferrous/ferric reaction was known to be catalyzed by trace levels of anionic impurities, and precautions were taken in the experiments to avoid this effect. A catalytic effect on the Fe^{2+}/Fe^{3+} electron-transfer rates was observed after a single layer of copper had been plated on a gold working electrode. This effect was believed to result from the fact that the solvated ion could approach the plated surface more closely than the gold electrode.

Studies were extended to the Cu^{2+}/Cu electrode reaction, which entails two consecutive electron transfers followed by incorporation of a copper atom into the metal phase. There were two reasons for selecting this reaction for study: (1) copper deposition had been one of the most troublesome cathodic reactions in the corrosion of LWR cooling systems, and (2) the system presented a special challenge in the extension of the electron-transfer theory methods to an ion for which Jahn-Teller distortion of the hydration shell had to be accommodated. A computer modeling analysis indicated that it would be possible to measure both the fast and the slow steps of the Cu^{2+}/Cu reaction sequence. Work continued on theoretical models of Cu^{+} and Cu^{2+} ions in water. Preliminary experimental measurements on Cu^{2+}/Cu^{0} in perchloric acid solution reproduced some data in the literature. However, it became clear in the modeling studies that the calculated rate of the fast reaction in the two-step reaction sequence needed to be reevaluated.

Copper deposition is an important cathodic reaction during stress corrosion cracking in LWRs, and the mechanism was poorly understood. Experimental measurements confirmed earlier reports that the reaction rate is controlled by the Cu^{2+}/Cu^{+} charge-transfer step. It was also found that traces of chloride ion strongly catalyzed this reaction. The catalytic effect was attributed to the adsorption of chloride ions on the electrode surface and promotion of the charge transfer through an anion bridge. As the concentration of the chloride ion was increased, the exchange current density of the Cu^{2+}/Cu^{+} step doubled, while that of the Cu^{+}/Cu step remained essentially constant. When the importance of the chloride catalytic effect was recognized, rigorous purification procedures were applied to the perchloric acid solutions, and the rate constant of the reaction decreased by two orders of magnitude. In later studies, experimental measurements indicated that the rate of the Cu^{2+}/Cu^{+} charge-transfer reaction increased about a hundred fold when the temperature was raised from 25°C to 200°C. An Arrhenius plot for the temperature dependence of this reaction resulted in an activation energy of 30 kJ/mol.

In 1997, the kinetic studies of the Cu^{2+}/Cu electrode reaction were completed. The high-temperature/high pressure studies of the Cu^{2+}/Cu^{+} reaction, which is the rate-determining step in the overall copper deposition/dissolution process, were extended from a maximum temperature of 100°C to 200°C. The activation energy was found to be 32 ± 5 kJ/mol, and the transfer coefficient was independent of temperature.

In 1994, a collaborative effort with the ANL Materials Science Division was continued on the use of synchrotron X-ray methods to probe electrified interfaces that were buried under or within condensed phases. X-ray reflectivity techniques had been used to look at the metal side of the interface and the structure of the solution side of the electrical double layer. A similar approach was undertaken, using a complementary technique involving X-ray standing waves (XSW). This combination of techniques permitted studies of the double layer over a concentration range of five orders of magnitude at a distance from the electrode surface ranging from a few angstroms to tens of thousands of angstroms. A special thin-layer, X-ray/electrochemical cell capable of XSW measurements was developed. This apparatus was used to study incipient pore formation in luminescent silicon layers, which were of interest for future industrial applications due to their luminescence at visible frequencies.

Ultracapacitor Studies. A new program was started recently on the surface phenomena involved in ultracapacitor energy-storage devices. The characteristics of these devices are between those of classical "dielectric" capacitors and those of batteries. The capacity of ultracapacitors stems from three phenomena: (1) the capacitance of the electrical double layer, (2) the adsorption/desorption pseudocapacitance, and (3) the capacitance caused by oxidation/reduction processes of the electrode material occurring at or near the interface.

All of these phenomena can be investigated by means of synchrotron X-ray techniques, and initial studies are in progress on RuO_2 surfaces because this oxide, alone or with other oxides, is one of the most promising candidates for this application.

Theoretical Studies of Electrode Reactions. The investigations performed under this task were concerned with the more theoretical aspects of the electrochemical studies, but were so closely intertwined with the work in the preceding section that a separation may be rather artificial. Much of this work was done in cooperation with John Halley, a member of the Corrosion Institute at the University of Minnesota.

Theoretical models were developed for Cu^+ and Cu^{2+} ions in water. These were necessary for studying the Cu^+/Cu^{2+} electron-transfer process. A pair potential was derived for Cu^+/H_2O from *ab initio* molecular orbital calculations. This potential, with one derived previously for Cu^{2+}/H_2O, was tested successfully in molecular dynamics simulations of these ions in water. Two- and three-body interaction energies were calculated for tetrahedral, octahedral, and cubic arrangements of H_2O molecules around Cu^+ and Cu^{2+} ions in $[Cu(H_2O)_n]q^+$ clusters. Previous studies of copper ions in water had not taken into account the Jahn-Teller distortion of water in the first solvation shell about Cu^{2+}. X-ray diffraction data indicated that this distortion is significant and must be included in accurate calculations. Some disagreement had arisen as to the stability of metallic copper (Cu^0) in water. High-level calculations indicated that the interaction energy was very small (<0.2 eV).

In further studies of $Cu^{2+}(H_2O)_n$ clusters, the molecular dynamics results did not jibe with those from neutron-diffraction experiments. A possible explanation was a difference in the aqueous solutions used in the work. Detailed calculations were performed to elucidate the mechanism of the $Cu^{2+} + 2\,e^- \rightarrow Cu^0$ reaction in water. Molecular modeling studies of the electron-transfer reaction involved the multibody interactions of $Cu^{2+}(H_2O)_n$ clusters.

The electron-transfer rates are dependent upon electron coupling and a weighted density of states. The electronic coupling was calculated for three possible electron-transfer reactions in the copper deposition: (1) direct interaction, (2) outer-sphere electron transfer (water-water bridge), and (3) inner-sphere electron transfer (chloride bridge). The greatest coupling was found with the chloride bridge as a result of the shorter copper-copper distance rather than intrinsic chemical effects. Research continued in this area on the effects of other anions on the electronic coupling in Cu^{2+}/Cu^0 electron-transfer reactions. Electronic couplings for bromine- and fluorine-bridged reactions were similar to those for water-water bridged reactions. In 1996, investigations were conducted on the homogeneous inner-shell electron-transfer reaction $Fe^{3+} + e^- \rightarrow Fe^{2+}$ with the bridging halide anions, F^-, Br^-, and I^-. These anions gave increased electronic coupling due to a closer approach distance than is possible for an outer-sphere water bridge.

Personnel. These programs were under the general direction of Vic Maroni. Other CMT staff personnel contributing to this work included Wally Calaway, Larry Curtiss, Stan Johnson, Xiandong Feng, Carlos Melendres, Zoltan Nagy, George Papatheadorou, Gerry Reedy, and Ben Tani. This, like most of the other basic programs, made use of postdocs and other temporary personnel.

POLYMER ELECTROLYTES

This project is a fundamental study of lithium polymer electrolytes used in lithium batteries. The studies focus on the effects of the polymer host on ion pairing, which strongly affects the ionic transport in these systems. In recent work, *ab initio* molecular orbital theory has been applied to the energetic, structural, and dynamical properties of ion-ion and ion-polymer interactions at the molecular level, in combination with molecular dynamics simulations performed at the University of Minnesota. It was found that the binding energies of lithium cation complexes with alkyl oxide chains increase with coordination of the cation by oxygen, while the binding energy of the Li-O bond decreases. This theoretical study was conducted by Larry Curtiss.

GEOCHEMISTRY

The geochemistry research work was focused initially on two areas: (1) geochemistry and evolution of hydrothermal systems associated with volcanic areas, and (2) isotopic and organic geochemistry of carbon in sedimentary basins. In 1992, a more basic effort was added on mineral-fluid interactions.

Hydrothermal Systems. The extent of disequilibrium between ^{238}U and ^{230}Th was used to investigate the rates and mechanisms of element redistribution and the time scale of hydrothermal activity. One application was to determine the ages of travertine deposits in the northern part of Yellowstone Park. Travertines are calcium carbonate deposits that are formed when saturated or supersaturated groundwater emerges at the Earth's surface. The alpha decay rate of ^{234}U (half-life = 245,000 y) to ^{230}Th (half-life = 75,400 y) provided a "clock" for determining the age of the travertine, which contained a negligible amount of ^{230}Th when it was formed, so the $^{230}Th/^{234}U$ ratio is essentially zero. The time for the ^{234}U and ^{230}Th to reach equilibrium is about 500,000 y. The age of the travertine can thus be determined from the $^{230}Th/^{234}U$ activity ratio, with an upper limit of about 500,000 y. By using this approach, travertine formation was shown to have occurred about 130,000 to 170,000 years ago. This type of information should lead to a better understanding of the timing of the last glaciation in the region and the underlying thermal systems. These studies were done in collaboration with Kenneth Pierce of the U.S. Geological Survey and M. T. Murrell, a geochemist at Los Alamos National Laboratory (LANL).

Further studies of the Yellowstone Park area included the geochemistry and isotopy of radium in the hydrothermal systems. The radium concentration proved to be controlled by barite saturation and zeolite-water ion exchange.

Other field-based studies showed that the ages of silica samples from volcanic areas in the northern Kenya Rift Valley correlated with high paleolake levels, which were associated with humid climatic periods during the past 150,000 years. The main significance of this work is that it showed clearly, for the first time, the influence of climatic variations on geothermal activity in a continental rift zone.

Thermal springs along the shores of the Gulf of Suez and along the Nile River just south of Cairo were sampled for chemical and isotopic analysis in a collaborative study with Egyptian colleagues from Washington University and the Egyptian Geological Survey and Mining Authority. The objective was to determine the geothermal potential of these areas and their hydrogeochemical characteristics. The results showed that the Egyptian thermal waters contain water from either the Nubian sandstone aquifer or the Nile River, derived their solutes from Tertiary marine sedimentary rocks, and were heated conductively at depths of 3 to 4 km under a normal regional thermal gradient.

Mineral-Fluid Interactions. In 1992, a new project was initiated on the application of synchrotron radiation techniques to *in situ* studies of mineral-fluid interactions. A special X-ray-transparent cell that was developed for these studies is illustrated in Fig. 6-37. The cell performed well in tests at the National Synchroton Light Source at Brookhaven National Laboratory, and initial studies were made on changes in the surface structure of calcite during dissolution and growth. These experiments on a calcite/fluid interface indicated that the structure of the calcite cleavage surface during dissolution was determined by the near-ideal, atomic-scale termination of this surface and the long-range atomic order of the underlying bulk crystal. A multistep mathematical model was developed to characterize the surface.

X-ray reflectivity and diffraction measurements were used to characterize an ovatite over-growth as it was precipitated from aqueous solution onto a calcite cleavage surface. Scans were made during 4,585 min (76.4 h) of growth. Reflectivity was used to determine the properties of thin films, including the thickness, interfacial roughness, and real-space electron density profile across interfaces. A growth rate of 15 Å/h during the first 540 min decreased considerably thereafter. An analysis of the results from these measurements indicated that the ovatite had grown heteroepitaxially on the calcite cleavage surface.

X-ray standing wave measurements were made at mineral-water interfaces to provide information on the structures of metal adsorbates. Such information is needed to understand contaminant transport in ground-water aquifers. When lead was adsorbed from an aqueous solution onto the (104) cleavage surface of calcite, and the solution was then removed, approximately a 5% monolayer of lead was found adsorbed on the calcite. This lead occupied the same position as calcium relative to the (104) lattice plane. Additional experiments were conducted with solutions containing known concentrations of uncomplexed Pb^{2+} or $PbOH^{+}$ ions that were available for adsorption on the calcite surface. The conclusions from these experiments were:

1. About 5-17% of a monolayer equivalent of lead was adsorbed from the solution onto the calcite surface.
2. The amount adsorbed was independent of time from 8 to 93 h of reaction.
3. The lead occupied calcium sites.
4. The coverage and ordering of lead were about the same for *in situ* and *ex situ* measurements.
5. The adsorbed lead was stable in both aqueous solution and flowing helium for the duration of the measurements (about 96 h).

Isotope and Organic Geochemistry. A new gas chromatography/isotope ratio mass

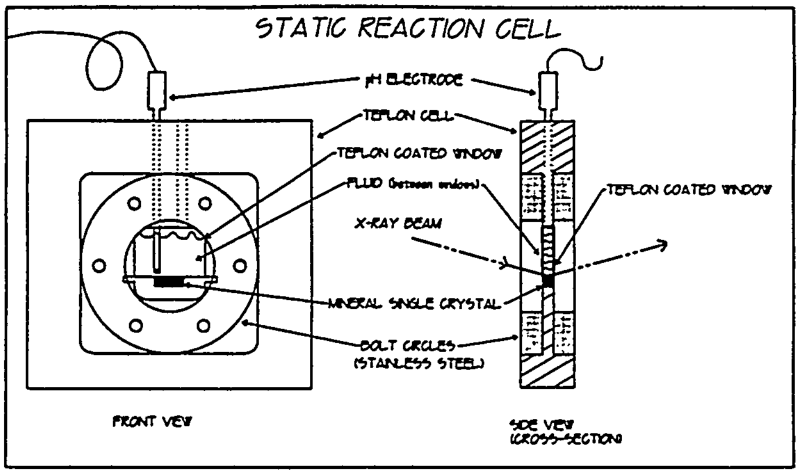

Fig. 6-37. Reaction Cell for Studies of Mineral-Fluid Reactions

spectrometer (GC/IRMS) was acquired, and a research program was undertaken in which this instrument was used for compound-specific carbon isotopic analysis in studying petroleum geochemistry. Suites of well-characterized petroleum samples were obtained from scientists at major oil companies, the U.S. Geological Survey, the Illinois Geological Survey, and several universities. Each suite was selected to address one or more of the following questions: (1) the relationship between source rock quality and the depositional environment, (2) the relationship between oil composition and source rock type, (3) the nature of chemical changes that occur within organic matter during diagenesis and catagenesis, (4) the effects of migration, mixing, and biodegradation on oil composition, and (5) the validity of oil-source rock and oil-oil correlations. Before analyzing the samples, CMT researchers spent considerable effort to test the GC/IRMS procedure, using n-alkanes of known carbon isotopic composition.

The carbon isotopic compositions of n-alkanes in oil samples from different reservoirs in an oil field near Phillipstown, Illinois, were similar. This finding is consistent with biomarker data indicating that these oils were generated from a similar source rock, but they appeared to have undergone varying degrees of biodegradation.

Although the chemical and isotopic compositions of hydrocarbon compounds in petroleum had been well studied, the geochemistry of nitrogen compounds in petroleum was another story. Therefore, some studies were conducted on nitrogen-rich crude oils in California. Nitrogen isotope determinations on 25 well-characterized nitrogen-rich crude oils showed that the sulfur-rich oils derived from marine-dominated organic matter had relatively low ^{15}N contents, while the sulfur-poor oils from organic matter containing some terrigenous material was high in ^{15}N. Variations in the nitrogen isotopic compositions were attributed to differences in the depositional environment, rather than to biodegradation or maturation processes.

Personnel. This effort, as in the past, was led by Neil Sturchio, and it included Teofilo Abrajano, Greg Archart, Allen Bakel, Ron Chiarello, Ben Holt (STA), Wally Calaway, Pete Lindahl, and Francis Markun, and several postdocs were also involved in certain aspects of the work. This was a highly collaborative program with many other institutions, several of which are in foreign countries.

ENHANCED METALLURGICAL PROCESSES

A small effort was continued on the use of molten sulfide mixtures to extract copper from scrap steel. For the production of sheet steel from scrap, the copper content of the material must be reduced to a level below 0.1 wt%. Measurements were performed at temperatures of 1365-1400°C on high carbon steel in equilibrium with mattes consisting of 80-90 wt% Al_2S_3, 10-20 wt% FeS, and 0-10 wt% MgS or CaS. For a steel/matte weight ratio of 4, the copper contents of the steel ranged from 0.04 to 0.09 wt%, where the initial values were 0.4 wt%. This procedure met the requirement of <0.1 wt% in the product, but required a large amount of matte. Investigations were then started on possible silicate-based slags that would remove copper from the steel, since silicate slags are already used widely in the industry.

Molten salts were also developed for the removal of lead from solid brass and copper surfaces. Treatment with the molten salts removed >90% of the surface lead from polished lead-bearing brass. Tests of treated brass samples by the EPA showed that this method of lead removal could be used for the pretreatment of brass parts in water systems.

This work, led by Milt Blander, was done by temporary personnel.

Analytical Chemistry Laboratory (ACL)

The Analytical Chemistry Laboratory continued to operate much the same as before, serving the Division, other projects at the Laboratory, various Federal agencies, and some private organizations. Dave Green continued to manage the organization. Fred Martino provided technical and quality assurance support for ACL and was the ANL Quality Assurance Representative for the Division. He was also responsible for a variety of administrative functions for ACL. Dave has become recognized as an authority on management of an analytical laboratory, and he has addressed various aspects of the subject in seminars and publications.

The organization consists of four groups—Chemical Analysis, Instrumental Analysis, Organic Analysis, and Environmental Analysis. The Group Leaders, respectively, are Don Graczyk, Del Bowers, Amrit Boparai, and Peter Lindahl. The ACL, like the rest of the Division, felt the effects of a shrinking budget. From 1990 to 1998, the technical staff level of the ACL decreased from about 50 to 35 or so. During that period, there was also a shifting emphasis in the nature of the analytical work that was needed. In the early 1990s, processing and recycling of IFR fuel was a major development effort that required extensive analytical work to evaluate the performance of the process operations. At the time that the IFR program was terminated, there was a rapidly growing interest in environmental and waste processing programs. The Division's programs up to that time had been concerned largely with inorganic and metallurgical materials. Many of these new program areas involved organic chemistry, and the ACL responded with a wide variety of new analytical capabilities for organic materials.

Upgrading and expansion of the ACL facilities and equipment continued in the 1990s. A computer-assisted bar code system was adopted for sample tracking and handling. A new laboratory was made available for analytical work on radioactive organic samples. In 1993, quality assurance and control procedures were developed to satisfy DOE and EPA reporting requirements. Among the new equipment items were a microwave digestion system, an automated C/H/N analyzer, a new mass spectrometer for organic analysis, an interfacing liquid chromatography/mass spectrometer for determining organic compounds, an inductively coupled plasma/mass spectrometer, a laboratory robotics system, a mercury analyzer, an oxygen combustion vessel for determining trace metals in water and environmental samples, a liquid scintillation counter for α and β activity, a germanium detector for γ-emitting nuclides, an upgraded scanning electron microscope user facility, a new X-ray diffractometer system, and Fourier transform infrared and Raman spectrometers.

In 1996, the ACL, as mentioned earlier, placed a home page on the Internet, which can be accessed on the World Wide Web by the address:

www.cmt.anl.gov/acl/acl.htm

This page is well done and contains a lot of information about the organization, as well as a color picture of the staff members.

The following is a selected list of the activities of the ACL in the 1990s; many of these relate to other CMT programs that were described earlier. This list gives a good sense of the wide range of ACL capabilities.

Engineering Studies of Pyrochemical Processes for Integral Fast Reactor Fuels
Rare-Earth Characterization Studies
Zeolite Immobilization of IFR Waste Salt
Studies of Alkalis in Hot Off-Gas from Pressurized Fluid-Bed Combustors
Analysis of Environmental Samples
Isolation of Strontium from Geological Samples for Isotopic Analysis
Plutonium Residue Recovery Program
Decomposition Products from Thermally Unstable Complexants
Molten Corium-Concrete Interaction Studies
Preparation of Samples for the National Energy Agency Committee on Reactor Physics Study
JANUS Water Analysis
Plutonium (VI) Speciation Study
Analysis of Cotton and Waters
ANL-West Soils, Vegetations, and Waters
Radiation Damage Studies for Superconductive Super Collider Detector Research
Synchrotron Thrust Group Activities
Radiological Environmental Analyses for Rocky Flats Plant
Analysis of Cores from Pressure Vessel of Experimental Boiling Water Reactor
Analytical Support Using X-Ray Diffraction and Scanning Electron Microscopy
Fourier Transform Infrared Microscopic Analysis of Fluid Inclusions
Studies of Organic Fluid Fouling in Heat Exchange Systems
Fourier Transform Infrared (FTIR) Analysis of Semivolatiles in Soils
Remote Detection of Chemical Agents with FTIR
Incinerator Monitoring for Organic Analytes
Determination of Volatile Organic Compounds for Lake Michigan Study
Walter Reed Army Institute of Research Site Characterization
Method Development and Testing for EPA
High Performance Liquid Chromatography Separation of Explosive and Other High Molecular Weight Compounds
Supercritical Fluid Chromatography/Matrix Isolation-Infrared Spectroscopy
Competitive Exchange Experiments in IFR Chemical and Engineering Support Studies
X-Ray Diffraction Studies of Zeolite Materials
Phase Composition/Solubility Studies on Equilibrated Mixtures of LiCl and KCl in Water
Procedures for Determining Uranium and Uranium Isotopes in High Silica Soils
Battery Program Support

Analysis of a Novel Neutron Absorber
Study of N_2O Emissions from Fluidized Bed Combustors
Environmental Monitoring Program
National Acid Precipitation Assessment Program
ANL Geoscience Programs
Radium Measurements (Geochemical)
Rocky Flats Environmental Restoration Program
Radiochemical Analysis of Experimental Boiling Water Reactor Vessel
Detection of Illegal Drug Laboratories
Computer Generation of Reporting Forms for Volatile Organic and PCB/Pesticide Environmental Analysis
Analysis of Waste Isolation Pilot Plant (WIPP) Samples by the Solid Adsorbent Method
Analytical Method Development for WIPP
Canister Cleaning and Certification for the WIPP
Analysis of Headspace Gases for the WIPP
Supercritical Fluid Extraction/Gas Chromatography for Analysis of Organic Compounds
Analysis of Environmental Samples for the U.S. Department of Agriculture
Environmental Assessment Study for Contaminants at Hohenfel Training Area Site, Germany
Development of Infrared Aerosol Analyzer
Support for CMT Nuclear Waste Programs
Monitoring of Antimony Levels in Scrap Aluminum
Chemical Transformation of Isotopically Enriched Tin Oxide
Advanced Photon Source Component Materials
Grafenwöhr Soil Samples
Stability of Calibration Standards for ICP/AES
Radiochemical Method Evaluation and New Method Development
Applications of FTIR Microscope to Identification of Wastes, Spill Residues, and Contaminants
Characterization of Products from Automobile Shredder "Fluff" Recycling
Determination of Rare Earth Elements and Calcium in Autopsy Tissues
Determination of Platinum in Tissues
Determination of ^{226}Ra in Human Tissues
Isolation of Uranium and Thorium from Soils for Isotopic Analysis
Characterization of Nitrogen in Lime-Scrubber Waste
Properties of High-Temperature Superconductors
Identification of Hazardous Wastes
Development of Integrated Performance Evaluation Program
Determination of Americium in Environmental Samples
Rietveld Analysis of X-Ray Powder Diffraction Data
Stand-Off (Remote) Detection
Analytical Certification of IFR Special Reference Materials
Incinerator Monitoring
X-Ray Diffraction Support (ANL Programs)
Studies of TRU·Spec and RE·Spec Chromatography
Improved Methods to Determine Actinides in Environmental Samples
Animal Orphan Waste
Methodology for Characterizing Chlorofluorocarbons in Polyurethane Foam
Analysis of Nuclear Waste Glasses and Slags
Calcium Isotopic Determination in Canine Bone and Blood Serum
Automated Real-Time Analysis of Chemical Sensor Data

Analysis of Soils for Explosives
Treatment of Cesium-Contaminated Milk
Engineering Studies of Electrometallurgical Treatment of Nuclear Fuel
Thermal Treatment Systems for Organic Effluents
Characterization of Used HEPA Filters for Disposal
Development of "Smart" Chemical Sensors
Analytical Procedures for Waste Minimization and Pollution Prevention
Gross α/β Analysis of Environmental and Mixed-Waste Samples
Microwave-Assisted Extraction of Semivolatile Organic Compounds from Soil
Analysis of Highly Acidic Mixed Waste
Determination of Arsenic Species in Soil Samples from the Rocky Mountain Arsenal
Transition Metal Speciation in Textile Mill Wastewater
Determination of Uranium in Dissolver Solutions for Production of ^{99}Mo
Development of an Analytical Scheme to Determine Actinides in Soil
Methods for Determining Metals in Waste Oil
Support for High-Temperature Superconductor Development
Wastewater Treatability Studies
Measurement of Calcium Isotopic Ratios in Canine Blood Serum
Development of a Continuous Emission Monitor for Thermal Treatment Systems
Determination of Platinum in Inner-Ear Fluid of Guinea Pigs
Radon Remediation
Separation of Mercury from Americium for Radioactive Waste Analysis
Determination of Reaction Products from Molten Sodium and Chlorinated Hydrocarbons
Dissolution Procedure for Low-Enriched Uranium Metal Targets
Automated Target Recognition Using Multispectral Images
Project in Support of Counternarcotics Efforts
Development of Solid-Phase Extraction Disks for Radiochemical Analysis
Analysis of Samples from Process to Recycle Aluminum Salt Cake
Continuous Monitoring of Plasma Arc Furnace at ANL-West
Preparation of Simulated Solidified Waste Samples for WIPP Performance Demonstration Program
Automated Data Cataloging Procedure for Objects in AMPS Multispectral Imagery
Development of Method for Radium Determination in Aqueous Samples
Domestic Nuclear Smuggling Exercise
Development of a No-Moving-Parts FTIR Sensor
JANUS Reactor Characterization
Study of Dry-Storage Casks for Spent Nuclear Fuel

THE DIVISION'S FUTURE

One certainty about the future is that the Division will continue to face fierce competition in seeking and keeping funding for programs. This competition comes from industry, the universities, other national laboratories, independent research organizations, and even other divisions at ANL. It is also affected by the changing perceptions of national technical needs and budget pressures in Washington. The hope is that CMT will be able to meet this competition because of its excellent staff people, unique facilities, and extensive experience in a variety of research areas and technology development programs. In recent years, DOE funding of the Division's programs has declined, but much of the slack has been taken up by cooperative work with industries in the form of CRADAs (Cooperative Research and Development Agreements) and "work for others" agreements, which may involve other Government agencies or private organizations.

With the demise of the Integral Fast Reactor program and the ban on commercial fuel processing in the United States, program support on processes for the recovery of uranium and plutonium from spent nuclear fuel has vanished. In its stead are programs to treat spent fuels to separate transuranic (TRU) elements (neptunium, plutonium, americium, and curium) for disposal in a waste depository. Electrometallurgical processes show promise for this application if current throughput rates can be increased. Preliminary results suggest that it may be possible to fix TRU elements on a zeolite bed in a waste form suitable for repository disposal.

For over ten years the Division has been conducting a variety of tests on simulated waste glasses and spent reactor fuels under conditions similar to those in the Yucca Mountain Repository. An exciting recent discovery is that even though neptunium, on release from a waste form, will migrate rapidly through the volcanic tuff of a repository, it will be retained by alteration products, principally zeolites, that form on the surface of the glass by reaction with water vapor. This finding must be explored further. In addition, continuation of long-term (5- to 10-year) corrosion tests with waste samples would be desirable.

Throughout its history, the Division has been at the forefront of development work on advanced solvent-extraction processes and equipment. An exciting new development is aqueous biphase extraction, which shows promise for a wide range of applications. Typical examples are cleanup of industrial wastes and purification of low-grade ores such as bauxite for aluminum production. The Division intends to pursue this emerging technology vigorously because of its potentially great versatility.

The deregulation of electricity may bring about some major changes. Utilities are likely to reduce their involvement in the generation of electricity and concentrate on its distribution. Fuel cells operating on natural gas are expected to be finding increased use for local generation of electricity by cities, industrial organizations, office buildings, large housing complexes, and even homes. There is also much interest in the use of fuel cells in transportation applications, where they would most likely be used in hybrid vehicle systems. Competition will be heavy for funding to support research for these applications. The Division is well positioned to contribute to this effort due to its past work on molten carbonate and solid oxide fuel cells, and especially its leading-edge work in polymer-electrolyte fuel cells. The best opportunities for work on fuel cells may be where highly focused, sophisticated research efforts can be directed toward niche areas that need attention, rather than complete systems.

The situation with batteries is somewhat similar to that for fuel cells. The Division has had large programs on high-temperature lithium-alloy/metal sulfide batteries for electric vehicle propulsion and load leveling on electric utility systems. This technology was developed to the stage where it was ready for commercialization. The battery work evolved into a number of other areas, including sodium/metal chloride, lithium/polymer electrolyte, lithium-ion, and nickel/metal hydride systems. The lithium systems, in particular, have a potentially huge market in consumer electronics. Research in this field is highly competitive. The Division is enjoying considerable success in using sophisticated basic research tools to investigate the detailed chemistry and electrochemistry of these systems, and might have a similar role in other specialized areas of industrial research.

The Division has, for years, operated a large facility for conducting performance and cycle-life tests on a variety of commercial and experimental batteries. Diagnostic procedures for failure analysis or performance degradation are also conducted when needed. Indications are that similar testing of fuel cells may be a significant program

When the Division came into being in 1948, the staff consisted of many young scientists and engineers. Most if not all of these people have retired by now. The Division has been able to attract as replacements outstanding young graduates and has also hired distinguished leaders in particular areas of research. In addition, the Division makes extensive use of postdoctoral people who are seeking R&D experience. Some of these are retained when their appointments expire. The Division takes very seriously its responsibility to train young scientists to do imaginative, high-quality research.

The consensus is that the future of the Chemical Technology Division can be viewed with cautious optimism.

APPENDIXES

General References

American Nuclear Society, *Controlled Nuclear Chain Reaction: The First 50 Years*, American Nuclear Society, LaGrange Park, IL (1992).

Clarfield, Gerald H., and William M. Wiecek, *Nuclear America, Military and Civilian Nuclear Power in the United States 1940-1980*, Harper & Row, New York (1984).

Evans, H., S. Vogler, and H. H. Hyman, *Studies in Counter-Current Solvent Extraction for the Decontamination of Enriched Uranium from the Proposed High Flux Research Pile*, ANL-4110, Argonne National Laboratory (Jan. 28, 1948).

Fermi, Laura, *Atoms in the Family; My Life with Enrico Fermi*, University of Chicago Press, Chicago, IL (1954).

Gillette, Robert, "Nuclear Safety (I): The Roots of Dissent," *Science* **177**, 771 (1972).

Gillette, Robert, "Nuclear Safety (II): The Years of Delay," *Science* **177**, 867 (1972).

Goldschmidt, Bertrand, *The Atomic Complex: A Worldwide Political History of Nuclear Energy*, American Nuclear Society, LaGrange Park, IL (1982).

Groueff, Stephane, *Manhattan Project: The Untold Story of the Making of the Atomic Bomb*, Little, Brown & Co., Boston (1967).

Hewlett, Richard G., and Oscar E. Anderson, Jr., *The New World, 1939-1946*, Pennsylvania State University Press, University Park, PA (1962).

Hewlett, Richard G., and Francis Duncan, *Atomic Shield, 1947/1952, Vol. II, History of the United States Atomic Energy Commission*, Pennsylvania State University Press, University Park, PA (1969).

Holl, Jack M., *Argonne National Laboratory, 1946-96*, University of Illinois Press, Urbana & Chicago, IL (1997).

Johnson, Otto (ed.), *1997 Information Please Almanac*, Houghton Mifflin Company, Boston (1997).

Massachusetts Institute of Technology Faculty, Jack Dennis (ed.), *The Nuclear Almanac—Confronting the Atom in War and Peace*, Addison-Wesley, Reading, MA (1984).

Orlans, Harold, *Contracting for Atoms*, Brookings Institution, Washington, DC (1967).

Rhodes, Richard , *The Making of the Atomic Bomb*, Simon & Schuster, New York (1986).

Seaborg, Glenn T., *The Plutonium Story: The Journals of Professor Glenn T. Seaborg, 1939-1946*, Ronald L. Kathren, Jerry B. Gough, and Gary T. Benedict, eds., Battelle Press, Columbus, OH (1994).

Smith, Alice K., *A Peril and a Hope: The Scientists' Movement in America 1945-1947*, University of Chicago Press, Chicago, IL (1965).

Smith, Alice K., and Charles Weiner (eds.), *Robert Oppenheimer: Letters and Recollections*, Harvard University Press, Cambridge, MA (1980).

Smyth, Henry D., *Atomic Energy for Military Purposes*, Princeton University Press, Princeton, NJ (1945).

United Nations, *Proceedings of the Second United Nations International Conference on the Peaceful Uses of Atomic Energy*, September 1-15, 1958, United Nations, Geneva, Switzerland (1958).

Wright, John W., *The New York Times 1998 Almanac*, Penguin Putnam Inc., New York (1998).

Acronyms and Definitions

A

ABS	Aqueous Biphase Separation (process)
ACL	Analytical Chemistry Laboratory
ACS	American Chemical Society; American Ceramics Society
ACU	Advisory Committee on Uranium
ADF	Aqueous Dissolution Fluorination (process)
AEC	Atomic Energy Commission
AEM	Analytical Electron Microscopy
AES	Atomic Emission Spectrometry
AFBC	Atmospheric Pressure Fluidized Bed Combustion
AIChE	American Institute of Chemical Engineers
ALPR	Argonne Low Power Reactor
AMD	ANL Applied Mathematics Division
AMF	American Machine and Foundry
AMPEL	Argonne MHD Process Engineering Laboratory
AMPS	Apparatus for Monitoring and Purifying Sodium
ANL	Argonne National Laboratory
ANL-E	ANL-East (Illinois Site)
ANL-W	ANL-West (Idaho Site)
ANS	American Nuclear Society
APS	Advanced Photon Source
APST	Alkali Metal Particulate Sampling Train
ASR	Area Specific Resistance
ATR	Attenuated Total Internal Reflection (spectroscopy)
ATS	Alkali-Tin-Silicate Glass (for Pu)
AVIDAC	Argonne's Version of the Institute's Digital Automatic Computer

B

B&W	Babcock and Wilcox
BAPL	Bettis Atomic Power Laboratory
BASIC	A computer programming language
BBI	Breeder Blanket Interface
BCSC	Blanket Comparison and Selection Study
BET	Brunauer-Emmet-Teller (method of surface area analysis)
BNL	Brookhaven National Laboratory
BORAX	A series of ANL reactors used for safety research
BWR	Boiling Water Reactor

C

CAMD	Center for Advanced Microstructures and Designs
CANDU	Heavy water Canadian reactor
CCT	Coordinated Cluster Theory (for molecular structure)
CD-ROM	Compact Disk-Read Only Memory
CDC	Control Data Corporation
CDIF	Component Development and Integration Facility
CEN	ANL Chemical Engineering Division
CENHAM	A standardized glove-box design used in CMT
CFFF	Coal Fired Flow Facility
CHM	ANL Chemistry Division
Cintichem	Process used in Indonesia for ^{99}Tc Recovery
CIS	Conformal Ionic Solution Theory
CMPO	Extractant used in TRUEX process
CMT	ANL Chemical Technology Division
COBOL	A business-oriented computer language
COMMIX	Computer code for liquid metal feed system
CORCON	Thermal hydraulic code for source-term packages
CP	Chicago Pile (several reactors)
CPC	Compound Parabolic Collector
CPM	Critical Path Method
CRADA	Cooperative Research and Development Agreement
CRBR	Clinch River Breeder Reactor

CREX Solvent Extraction Process for Sr, Pb, Tc
CRSC Center for Research on Sulfur in Coal (Illinois)
CRT Cathode Ray Tube
CSDP Continental Scientific Drilling Program
CSEX Cesium Extraction Process
CSP Chloride Silent Power (British battery manufacturer)
CT ANL Components Technology Division
CTF Components Test Facility
CTIF Components Test and Integration Facility
CTIU Component and Test Integration Unit
CTR Controlled Thermal Reactor (program)

D

DADAC Dosimetry And Damage Analysis Center
DARPA Defense Advanced Research Projects Agency
DEC Digital Equipment Corporation
DIGICALC A computer program language
DOE Department of Energy
DRIFTS Diffusion Reflectance Infrared Fourier Transfer Spectroscopy
DTA Differential Thermal Analysis
DTRAM Dynamic Tritium Release and Analysis Model
DWPP Defense Waste Processing Plant

E

EADL Electrochemical Analysis and Diagnostics Laboratory
EBR Experimental Breeder Reactor
EBR-I Experimental Breeder Reactor No. I
EBR-II Experimental Breeder Reactor No. II
EBWR Experimental Boiling Water Reactor
ECN Netherlands Research Foundation
ED Electron Diffraction
EDAX Energy Dispersive X-ray Analysis
EDS Energy-Dispersive Spectroscopy (X-ray)
EDTA Ethylene Diamine Tetraacetic Acid
EELS Electron Energy Loss Spectroscopy
EES ANL Energy and Environmental Sciences Division
EIA Electrochemical Industrial Associates
EIS ANL Environmental Impact Studies Division
EMF Electromotive Force
ENG ANL Engineering Division
EPA Environmental Protection Agency
EPRI Electric Power Research Institute
ERC Energy Research Corp.
ERDA Energy Research and Development Administration
EROSION/MOD Computer Code for Erosion in FBC
ES ANL Energy Systems Division
ET ANL Energy Technology Division
ESCA Electron Spectroscopy for Chemical Analysis
ETF Engineering Test Facility (MHD)
EXAFS Extended X-ray Absorption Fine Structure

F

FACT Facility for the Analysis of Chemical Thermodynamics
FARET Fast Reactor Test Facility
FBC Fluidized Bed Combustion
FCF Fuel Cycle Facility (at ANL-W)
FE ANL Fuels and Energy Division
FEF Fuel Examination Facility (at ANL-W)
FEUL Fossil Energy Users' Laboratory
FFTF Fast Flux Test Facility
FLUFIX/MOD2 Computer Code for Fluidized Bed Hydrodynamics
FORTRAN A computer language
FTIR Fourier Transform Infrared (spectroscopy)

FWDC	Foster Wheeler Development Corp.
FY	Government Fiscal Year

G

GAC	General Advisory Committee
GC	Gas Chromatography
GCFR	Gas-Cooled Fast Reactor
GE	General Electric Co.
GPU	General Public Utilities Corp.
GTM	Generic TRUEX Model

H

HDPE	High Density Polyethylene
HEDL	Hanford Engineering Development Laboratory
HEPA	High Efficiency Particulate Air (filter)
HETP	Height Equivalent to a Theoretical Plate (or stage)
HEU	High Enriched Uranium
HFEF	Hot Fuel Examination Facility
HFIR	High Flux Isotope Reactor
HPLC	High Performance Liquid Chromatography
HSRC	Hazardous Substance Research Center
HTER	High Throughput Electrorefiner
HTGR	High Temperature Gas-Cooled Reactor
HTM	Hydrogen Titration Method
HWR-NPR	Heavy Water Reactor-NPR (see NPR)

I

IAEA	International Atomic Energy Authority
IBM	International Business Machines
ICCI	Illinois Clean Coal Institute
ICBM	Intercontinental Ballistic Missile
ICPP	Idaho Chemical Processing Plant
IEA	International Energy Agency
IFC	International Fuel Cells
IFR	Integral Fast Reactor
ILRR	Interlaboratory Reaction Rate (program)
INEEL	Idaho National Engineering and Environmental Laboratory
INEL	Idaho National Engineering Laboratory (now INEEL)
INOR	International Tokamak Reactor
IPMA	Ion Probe Microanalyzer
IPNS	Intense Pulsed Neutron Source
IR	Infrared
IR-100	Award by *Industrial Research Magazine*
IRMS	Isotopic Ratio Mass Spectrometry
ISOA	Intermediate State of the Art
ITER	International Thermonuclear Experimental Reactor

J

JAERI	Japan Atomic Energy Institute
JANAF	Joint Army-Navy-Air Force (thermodynamic reference tables)
JANUS	Reactor used at ANL for biological research
JCAE	Joint Committee on Atomic Energy
JPDR	Japan Power Demonstration Reactor

K

KAPL	Knolls Atomic Power Laboratory
KB	Kilobyte
KGB	Komitet Gosudarstrenney Bezopasnoski (Committee for State Security)

L

LAMPF	Los Alamos Meson Physics Facility
LAMPRE	Los Alamos Molten Plutonium Reactor Experiment
LANL	Los Alamos National Laboratory
LASL	Los Alamos Scientific Laboratory (now LANL)
LBL	Lawrence Berkeley National Laboratory
LEU	Low Enriched Uranium

LIPE	Lithium-Polymer Electrolyte (battery)
LITCO	Lockheed Idaho Technology Co.
LLNL	Lawrence Livermore National Laboratory
LM	Lanthanum Manganite (fuel cell cathode)
LMFBR	Liquid Metal Fast Breeder Reactor
LMFR	Liquid Metal Fuel Reactor
LMFT	Low-Mass Flow Train (at Coal Fired Test Facility)
LOFT	Loss Of Fluid Test
LPTL	Lithium Processing Test Loop
LSU	Louisiana State University
LWR	Light Water Reactor

M

MAP3S	Multistate Atmospheric Power Production Pollution Study
MASCOT	Computer code used for sodium trap design
MASS-11	A word-processing program
MAWS	Minimum Additive Waste Stabilization Program
MBO	Management By Objectives
MCCI	Molten Core-Concrete Interaction
MCFC	Molten Carbonate Fuel Cell
MCPU	Multiple Cycle Plutonium Utilization
MCT	ANL Materials and Components Technology Division
MD	Molecular Dynamics
MEDEC	Melt/Drain Evaporation Calcination Process
MERDC	Mobility Equipment Research and Development Command
MET	ANL Metallurgy Division (now SSS, MST and others)
METC	Morgantown Energy Technology Center
MeV	Million Electron Volts
MFTF	Mirror Fusion Test Reactor
MHD	Magnetohydrodynamics
MI	Matrix Isolation (spectrometry)
MIR	Russian Space Station
MISTT	Midwest Interstate Sulfur Transport and Transformation
MIT	Massachusetts Institute of Technology
MMS	Masked Multichannel Scaler
MNDO	Modified Neglect of Differential Overlap (molecular structure theory)
MNM	Metal-to-Nonmetal (transitions)
MOX	Mixed Uranium-Plutonium Oxide (reactor fuels)
MS	Mass Spectrometry
MS-DOS	Microsoft Disk Operating System
MSD	ANL Materials Science Division
MSID	Mass Spectrometric Isotopic Dilution
MSOFC	Monolithic Solid Oxide Fuel Cell
MSRE	Molten Salt Reactor Experiment (at ORNL)
MST	ANL Materials Science and Technology Division
MSW	Municipal Solid Waste
MTR	Materials Test Reactor
MTU	Mass Transfer Unit (in electrorefiner)
MW(e)	Megawatts Electrical (electricity produced by a reactor)
MW(t)	Megawatts Thermal (heat produced by a reactor)

N

N.S.	Nuclear Powered Ship (civilian)
NAA	Neutron Activation Analysis
NAPAP	National Acid Precipitation Assessment Program
NAS	National Academy of Sciences
NASA	National Aeronautics and Space Administration
NASICON	An experimental ionically conductive glass composition
NBL	New Brunswick Laboratory
NBS	National Bureau of Standards
NBTL	National Battery Test Laboratory
NDRC	National Defense Research Council
NEACRP	National Energy Agency Committee on Reactor Physics
NEPA	Nuclear Energy for Propulsion of Aircraft

NEPEX	Neptunium-Plutonium Extraction Process
NKVD	Predecessor of KGB (see)
NMFECC	National Magnetic Fusion Energy Computation Center
NMR	Nuclear Magnetic Resonance
NO_x	Generic term for nitrogen oxides, usually applied to air quality
NPR	New Production Reactor (for tritium production)
NPS	National Park Service
NRC	Nuclear Regulatory Commission
NRTS	National Reactor Testing Station (now INEEL)
NRX	Reactor at Chalk River, Canada
NSLS	National Synchrotron Light Source (at BNL)
NTA	Nitrilotriacetic Acid

O

O/M Ratio	Oxygen-to-Metal Ratio
OEPM	Office of Electrochemical Project Management
OPEC	Organization of Petroleum Exporting Countries
ORACLE	Oak Ridge Automatic Computer Logical Engine
ORNL	Oak Ridge National Laboratory
ORR	Oak Ridge Research Reactor
OSRD	Office of Scientific Research and Development

P

PAD	ANL Particle Accelerator Division
PAFC	Phosphoric Acid Fuel Cell
PAH	Polycyclic Aromatic Hyrdrocarbons
PAHR	Post-Accident Heat Removal
PASCAL	A computer language
PC	Personal Computer
PCB	Polychlorinated Biphenyl
PDP	Model of Digital Equipment Corp. computer
PEFC	Polymer Electrolyte Fuel Cell
PEG	Polyethylene Glycol
PEMFC	Polymer Exchange Membrane Fuel Cell
PEO	Polyethylene Oxide
PERT	Program Evaluation and Review Technique
PFBC	Pressurized Fluidized Bed Combustion
PFP	Plutonium Finishing Plant
PIFAG	Production Irradiated Fuel Assay Gauge
PL/1	A computer language
PNL	Pacific Northwest Laboratory
POB	Proof of Breeding
PPG	Polypropylene Glycol
PRDC	Power Reactor Development Corporation
PuRR	Plutonium Residue Recovery
PVC	Polyvinyl Chloride
PWR	Pressurized Water Reactor
PYRO	Computer Model for IFR Process

Q

QA	Quality Assurance; ANL Quality Assurance Division
Quad	One quadrillion (10^{15}) Btu

R

RABSAM	Regenerable Activated Bauxite Sorber Alkali Monitor
RAM	Random Access Memory
RAS	ANL Reactor Analysis and Safety Division
RBMK	Pressurized water reactor of Russian design
RDF	Refuse Derived Fuel
RDT	Reactor Development and Technology (an AEC division)
RE	ANL Reactor Engineering Division; Rare Earths
RERTR	Reduced Enrichment for Research and Test Reactors
RFP	Rocky Flats Plant
RMC	Reverse Monte Carlo
ROM	Read Only Memory

RTNS Rotating Target Neutron Source

S

SACRD Safety Analysis Computerized Reactor Data
SAFT Societe des Accumulateurs Fixe et de Traction
SASPE Algorithm for Speciation and Partitioning Equilibria
SASSE Algorithm for Stagewise Solvent Extraction
SCAQMD California South Coast Air Quality Management
SCTI Sodium Components Test Installation
SEM Scanning Electron Microscopy
SEM/EDS Scanning Electron Microscopy/ Energy Dispersive Spectrometry
SERI Solar Energy Research Institute
SFC Supercritical Fluid Chromatography
SIBELIUS Joint CMT-European Study of Ceramic Fusion Breeder Blankets
SIR Sodium Intermediate Reactor
Site A Site of CP-2 in Argonne Woods of Palos Park Forest Preserve
Site D Current Location of ANL in DuPage County
Site W Hanford, Washington
Site X Oak Ridge, Tennessee
Site Y Hanford, Washington
SNAP Systems for Nuclear Auxiliary Power (in space satellites)
SNL Sandia National Laboratories
SNM Special Nuclear Materials
SOFC Solid Oxide Fuel Cell
SOLGASMIX Computer code for calculating equilibrium gas compositions
SPACE Worksheet calculation for plant equipment size, plant space, costs
SPECTER Computer code for radiation damage
SPM ANL Special Materials Division
SPR Single-Pass Reactor
SREX Strontium Extraction Process
SRL Savannah River Laboratory (now SRNL)
SRNL Savannah River National Laboratory
SRP Savannah River Plant
SRTALK ORNL-PNL Solvent Extraction Process for Sr, Tc, Cs extraction
SS Stainless Steel
SSC Superconducting Super Collider
SSS ANL Solid State Science Division
SSTR Solid State Track Recorder
STA Special Term Appointment
STARFIRE A commercial fusion reactor concept (ANL)
STEP Source Term Experiments Program
STR Submarine Thermal Reactor

T

TBP Tributyl Phosphate
TCA 1,1,1-Trichloroethylene
TCE Trichloroethylene
TD ANL Technology Development Division
TEM Transmission Electron Microscopy
TEPR Tokamak Experimental Power Reactor
T_EX A word processing computer program
TGA Thermogravimetric Analysis
THORP Thermal Oxide Reprocessing Plant
TMI Three Mile Island
TNS The Next Step (a nuclear fusion reactor concept)
TPD Temperature Programmed Desorption
TREAT Transient Reactor Test Facility
TRIO Tritium Recovery In Pile
TRU Transuranium or transuranic
TRUEX Transuranium Extraction (process)
TSTA Tritium Systems Test Assembly
TVA Tennessee Valley Authority

U

UCLA	University of California at Los Angeles
UI-UC	University of Illinois at Urbana-Champaign
USABC	United States Advanced Battery Consortium
U.S.S.	U. S. Navy Ship
U.S.S.R.	Union of Soviet Socialist Republics
UKAEA	United Kingdom Atomic Energy Authority
UTC	United Technologies Corp.

V

VAX	Model of Digital Equipment Corp. computer
VRLA	Valve-Regulated Lead-Acid (battery)

W

WIPP	Waste Isolation Pilot Plant
WRAIR	Walter Reed Army Institute of Research
WSRC	Westinghouse Savannah River Co. (type of glass)
WVDP	West Valley Demonstration Plant (type of glass)
WWII	World War II

X

X-10	Clinton Laboratory at Oak Ridge
XANES	X-ray Absorption Near-Edge Spectroscopy
XRD	X-Ray Diffraction
XSW	X-ray Standing Waves

Y

Y-12	Isotope Separations Plant at Oak Ridge
YSZ	Yttria-Stabilized Zirconia (fuel-cell electrolyte)

Z

ZGS	Zero Gradient Synchrotron
ZPPR	Zero Power Plutonium Reactor
ZPR	Zero Power Reactor
ZSM-5	Type of zeolite

Subject Guide

APPENDIXES

Name Index

[1] Names of non-ANL personnel in italics.